bioRxiv preprint doi: https://doi.org/10.1101/511048; this version posted January 3, 2019. The copyright holder for this preprint (which was not certified by peer review) is the author/funder, who has granted bioRxiv a license to display the preprint in perpetuity. It is made available under aCC-BY 4.0 International license.

A staphylococcal cyclophilin carries a single domain and unfolds via the formation of an intermediate that preserves cyclosporin A binding activity

Soham Seal[1], Soumitra Polley[1], and Subrata Sau[1]*

[1]Department of Biochemistry, Bose Institute, Kolkata, West Bengal, India.

*Corresponding author: subratasau@gmail.com

bioRxiv preprint doi: https://doi.org/10.1101/511048; this version posted January 3, 2019. The copyright holder for this preprint (which was not certified by peer review) is the author/funder, who has granted bioRxiv a license to display the preprint in perpetuity. It is made available under aCC-BY 4.0 International license.

Abstract

Cyclophilin (Cyp), a peptidyl-prolyl *cis-trans* isomerase (PPIase), acts as a virulence factor in many bacteria including *Staphylococcus aureus*. The enzymatic activity of Cyp is inhibited by cyclosporin A (CsA), an immunosuppressive drug. To precisely determine the unfolding mechanism and the domain structure of Cyp, we have investigated a chimeric *S. aureus* Cyp (rCyp) using various probes. Our limited proteolysis and the consequent analysis of the proteolytic fragments indicate that rCyp is composed of one domain with a short flexible tail at the C-terminal end. We also show that the urea-induced unfolding of both rCyp and rCyp-CsA is completely reversible and proceeds via the synthesis of at least one stable intermediate. The secondary structure, tertiary structure, and the hydrophobic surface area of no intermediate are fully identical to those of other intermediate or the related native protein. Further analyses reveal no loss of CsA binding activity in rCyp intermediate. The thermodynamic stability of rCyp was also significantly increased in the presence of CsA, recommending that this protein could be employed to screen new CsA derivatives in future.

bioRxiv preprint doi: https://doi.org/10.1101/511048; this version posted January 3, 2019. The copyright holder for this preprint (which was not certified by peer review) is the author/funder, who has granted bioRxiv a license to display the preprint in perpetuity. It is made available under aCC-BY 4.0 International license.

Introduction

The cyclophilins (EC: 5.2.1.8) represent a family of highly conserved peptidyl-prolyl *cis/trans* isomerase (PPIase) enzymes those are expressed by most living organisms, and some giant viruses [1-5]. These proteins control protein folding by catalyzing the *trans* to *cis* isomerization of the peptidyl bonds those precede proline residues. These enzymes also influence numerous other cellular processes including protein trafficking, transcription, cell differentiation, apoptosis, protein secretion, T-cell activation, and signal transduction. In addition, these folding catalysts play critical roles in developing cardiovascular diseases, rheumatoid arthritis, viral infections, cancer, diabetes, sepsis, asthma, aging, neurodegenerative diseases, and microbial infections [2, 3, 6-11]. The catalytic activities of the cyclophilins are typically inhibited by cyclosporin A (CsA), a cyclic peptide harboring eleven amino acid residues [1]. A ternary complex, formed by the association of CsA-cyclophilin complex with calcineurin, prevents the dephosphorylation of the transcription factor NF-AT that, in turn, blocks the expression of cytokines from T-lymphocytes [12-14]. The reduction of T-cell activity by CsA has made it extremely useful in clinics, particularly for preventing the graft rejection after organ and bone marrow transplantation [2]. However, the severe side effects of CsA have restricted its use [15] and promoted to develop many CsA analogs with no immunosuppressive activity [2, 10, 11, 16-18]. Some of these CsA analogs though yielded promising results have not been approved yet.

Cyclophilins, located in the cytosol and membrane or cell organelles, are composed of either single domain or multiple domains [1-3, 19]. The catalytic domains of cyclophilins have a β-barrel conformation that is constituted with eight anti-parallel β-

bioRxiv preprint doi: https://doi.org/10.1101/511048; this version posted January 3, 2019. The copyright holder for this preprint (which was not certified by peer review) is the author/funder, who has granted bioRxiv a license to display the preprint in perpetuity. It is made available under aCC-BY 4.0 International license.

strands, two-three α-helices, and several connecting loops [1, 20, 21]. Their hydrophobic active sites are made using the side-chains of amino acid residues from most of the β-strands and loops. While thirteen residues are required for binding CsA [1, 20- 22], eleven residues in the active site are involved in the binding of a tetrapeptide substrate [1, 23]. Of the residues, nine residues are used by both CsA and substrate for binding.

The linear polypeptide chains synthesized in the living cells become functional only when these molecules are folded into proper three-dimensional forms. To experimentally understand the mechanism of protein folding, native/denatured forms of proteins are gradually unfolded/refolded followed by monitoring their conformational changes using a suitable probe [24, 25]. The unfolding/refolding study usually indicates whether the folding of a protein occurs by a two-state or by a multi-state mechanism through the generation of no or multiple intermediates. Additionally, unfolding studies intimate about the stability of proteins in the presence of ligands or mutations [26-32]. Furthermore, such studies have greatly influenced many biotechnological fields including drug discovery [33-39]. The three-dimensional structures of the cyclophilins are conserved but their amino acid sequences are not identical [1-3], indicating that the unfolding mechanism of these proteins may be different. Thus far, unfolding mechanisms of only a few cyclophilins [40-43] were studied though these proteins were considered as the promising drug targets [2, 3, 10, 11].

Staphylococcus aureus, a pathogenic bacterium, harbors a putative cyclophilin (SaCyp)-encoding gene that is not induced by stress [44] or required for its growth [45]. The amino acid sequence of SaCyp shares adequate homology with those of cyclophilins from other organisms [42, 46]. A homology modeling study indicated the presence of a

bioRxiv preprint doi: https://doi.org/10.1101/511048; this version posted January 3, 2019. The copyright holder for this preprint (which was not certified by peer review) is the author/funder, who has granted bioRxiv a license to display the preprint in perpetuity. It is made available under aCC-BY 4.0 International license.

CsA binding site in SaCyp. Various experimental studies have collectively suggested that SaCyp is a PPIase, exits as a monomer, binds CsA, and plays a role in the *S. aureus*-mediated virulence [42, 46]. However, the catalytic activity of SaCyp later appears to be not critical for its pathogenesis [47]. The appearance and dissemination of the multi-drug resistant *S. aureus* strains across the globe today have necessitated the discovery of novel antistaphylococcal agents [48-50]. The structural and unfolding data of SaCyp may expedite the discovery of novel inhibitors (including new CsA derivatives) those would, in turn, be useful not only for treating staphylococcal infections but also other diseases. Recently, a study has indicated that the drug-bound or drug-unbound form of SaCyp unfolds via the generation of one intermediate in the presence of guanidine hydrochloride (GdnCl) [42]. In addition, there was a significant stabilization of SaCyp in the presence of CsA [42]. Proteins are sometimes denatured by a different pathway in the presence of different unfolding agent [51-54]. Thus far, the unfolding mechanism and stability of SaCyp have not been verified using other denaturants. The structural and functional properties of GdnCl-made SaCyp/SaCyp-CsA intermediate are also currently not known with certainty. Moreover, the predicted domain structure of SaCyp [42] has not been confirmed by any biochemical study. Herein, we have studied the domain structure and urea-induced unfolding of a recombinant *S. aureus* Cyp (rCyP) [42] using various probes. Our limited proteolysis data indicate that rCyp is a single-domain protein with a flexible tail at its C-terminal end. The urea-induced equilibrium unfolding of both rCyp and rCyp-CsA occurred via the synthesis of at least one stable intermediate. None of the intermediates has the properties of a molten globule [55]. Of the intermediates, rCyp intermediate has nearly full CsA binding activity.

bioRxiv preprint doi: https://doi.org/10.1101/511048; this version posted January 3, 2019. The copyright holder for this preprint (which was not certified by peer review) is the author/funder, who has granted bioRxiv a license to display the preprint in perpetuity. It is made available under aCC-BY 4.0 International license.

Materials and Methods

Materials

Many materials including acrylamide, anti-his antibody, alkaline phosphatase-goat anti-mouse antibody, ANS (8-anilino-1-naphthalene sulfonate), bis-acrylamide, chymotrypsin, CsA, Phenylmethane sulfonyl fluoride (PMSF), isopropyl β D-1-thiogalactopyranoside (IPTG), proteinase K, protein marker, trypsin, and urea were used in the present study. We bought these materials from different companies such as Sigma, SRL, and Merck. rCyp was purified by a standard procedure as earlier reported [42].

Basic protein techniques

The basic protein methods, namely, protein estimation, Western blotting, SDS-PAGE, and staining of polyacrylamide gel, were performed as reported [42, 56-58]. The theoretical mass of monomeric rCyp was determined by analyzing its sequence with ProtParam (web.expasy.org), a computational tool. The molar concentration of rCyp was estimated using both its theoretical mass and content in buffer B [42]. To produce rCyp-CsA, we incubated 10 μM rCyp in buffer B with 20 μM CsA for 30 min at 4°C [42].

Functional investigation

The PPIase activity of rCyp (120 nM) was evaluated by RNase T1 (ribonuclease T1) refolding assay as reported [29, 42]. Previously, our modeling study indicated that one *S. aureus* Cyp molecule binds to one molecule of CsA [42]. Considering similar interaction between rCyp and CsA, the related equilibrium dissociation constant (K_d) was estimated by a standard method [42] with minor modifications. Briefly, the intrinsic Trp fluorescence spectra (λ_{ex} = 295 nm and λ_{em} =300-400 nm) of rCyp (2 μM) in the presence of varying concentrations (0 - 4 μM) of CsA were recorded using a

bioRxiv preprint doi: https://doi.org/10.1101/511048; this version posted January 3, 2019. The copyright holder for this preprint (which was not certified by peer review) is the author/funder, who has granted bioRxiv a license to display the preprint in perpetuity. It is made available under aCC-BY 4.0 International license.

fluorescence spectrophotometer. The fluorescence intensity values (at λ_{max} =343 nm), extracted from the spectra, were rectified by deducting the related buffer fluorescence and by adjusting for volume changes. Lastly, the K_d value was estimated by fitting of the fluorescence data to a standard equation from GraphPad Prism (GraphPas Software Inc.).

Limited proteolysis

To know whether rCyp carries any domain, limited proteolysis of this protein was separately executed by different proteolytic enzymes using standard methods [58, 59]. Briefly, a buffer B [42] solution carrying rCyp (10 µM) and an enzyme (0.025 - 0.1 µM) was incubated at ambient temperature. At different time points, an aliquot (50 µl) was pulled out and mixed with an SDS gel loading dye [56]. All of the aliquots were boiled prior to their resolution by a Tris-glycine SDS-13.5% PAGE. After staining with Coomassie brilliant blue, the photograph of acrylamide gel was captured as stated [58].

To determine the molecular masses of rCyp fragments, a MALDI-TOF analysis (Bruker Daltonics, Germany) was performed mostly as stated earlier [59]. Briefly, rCyp was exposed to a proteolytic enzyme for 10-20 min followed by the termination of reaction using PMSF at a final concentration of 0.5 mM. To inactivate the enzyme, the reaction mixture was incubated with benzamidine sepharose for 30 min. The supernatant collected after centrifugation was dialyzed against a 20 mM NH_4HCO_3 containing buffer for 4 h at 4^0C. Finally, the supernatant obtained after centrifugation of the dialyzed sample was mixed with an equal volume of sinapinic acid. After drying the mixture on a sample plate, it was analyzed by an MALDI-TOF mass spectrometry. The yielded m/z

bioRxiv preprint doi: https://doi.org/10.1101/511048; this version posted January 3, 2019. The copyright holder for this preprint (which was not certified by peer review) is the author/funder, who has granted bioRxiv a license to display the preprint in perpetuity. It is made available under aCC-BY 4.0 International license.

155 spectra were used to calculate the molecular masses of the rCyp fragments using a
156 standard method [60].

157 Spectroscopic observation

158 To know about the different structural elements of rCyp and rCyp-CsA in buffer
159 B [42], the ANS fluorescence (λ_{ex} / λ_{em} = 360 / 400-600 nm), intrinsic tryptophan (Trp)
160 fluorescence (λ_{ex} / λ_{em} = 295 / 300-400 nm), near-UV circular dichroism (CD) (250-320
161 nm), and far-UV CD (200-260 nm) spectra of these proteins were recorded essentially as
162 described before [42, 51, 58]. We used 25 μM protein for the near-UV CD spectroscopy
163 and 10 μM protein for the far-UV CD or the fluorescence spectroscopy. The path length
164 of cuvette in the near-UV CD spectroscopy was 5 mm, whereas that in the far-UV CD
165 spectroscopy was 1 mm. The ANS concentration used in the study was 100 μM. The
166 fluorescence or CD intensity values were rectified by subtracting the reading of buffer
167 from the reading of buffer carrying protein.

168 Unfolding and refolding of proteins

169 To study the unfolding pathway of rCyp and rCyp-CsA, these proteins (10 μM
170 each) were exposed to varying concentrations (0-8 M) of urea for ~18 h at 4°C as stated
171 [51, 58]. Protein aliquots were always treated with the freshly prepared urea solution.
172 To understand the effects of denaturant on the different structures of proteins, the ANS
173 fluorescence, intrinsic Trp fluorescence, and the CD spectra of the urea-
174 treated/untreated proteins were recorded as described above. The spectroscopic signals
175 were corrected by deducting the reading of urea containing buffer from the reading of
176 the same buffer carrying protein.

bioRxiv preprint doi: https://doi.org/10.1101/511048; this version posted January 3, 2019. The copyright holder for this preprint (which was not certified by peer review) is the author/funder, who has granted bioRxiv a license to display the preprint in perpetuity. It is made available under aCC-BY 4.0 International license.

177 To check whether the proteins denatured by 7-8 M urea can refold upon removal
178 of urea, they were dialyzed against buffer B [42] prior to the recording of their Trp
179 fluorescence spectra as described [51]. The spectra of equal extent of both native and
180 unfolded proteins were also recorded for comparison. To see whether the refolded rCyp
181 is functional, we performed RNase T1 refolding as stated [42].

182 ## Transverse urea gradient gel electrophoresis

183 The unfolding of rCyp and rCyp-CsA were also monitored by a standard
184 transverse urea gradient gel electrophoresis (TUGE) with minor modifications [29, 51,
185 61]. Briefly, a gel having a 10 - 7% acrylamide gradient and a 0 - 8 M urea gradient was
186 made using a 10% acrylamide solution and a 7% acrylamide solution containing 8 M
187 urea. At 0 and 8 M urea, the concentrations of acrylamide were 10% and 7%,
188 respectively. After turning the solidified gel 90º, protein (60 µg) in an SDS-less loading
189 buffer [56] was loaded on its generated well. Electrophoresis and staining of the gel were
190 performed using standard procedures [57].

191 ## Analysis of unfolding data

192 To gather clues about the unfolding pathways and the stabilities of rCyp and
193 rCyp-CsA, the unfolding curves, produced using their spectroscopic and TUGE data,
194 were fit to either the two-state (N ↔ U) or the three-state (N ↔I↔U) equation using
195 GraphPad Prism as described [24, 25, 29, 58]. Of the yielded thermodynamic
196 parameters, C_m, urea concentration at the midpoint of unfolding transition (i.e. urea
197 concentration when $\Delta G = 0$), ΔG^W, free energy change in the absence of urea, m,
198 cooperativity parameter of unfolding, and $\Delta\Delta G$, the difference of free energy change
199 between rCyp-CsA and rCyp, were considered in the study. The fraction of unfolded

bioRxiv preprint doi: https://doi.org/10.1101/511048; this version posted January 3, 2019. The copyright holder for this preprint (which was not certified by peer review) is the author/funder, who has granted bioRxiv a license to display the preprint in perpetuity. It is made available under aCC-BY 4.0 International license.

protein molecules was determined from the unfolding data using a standard method [29].

Results

Domain structure of rCyp

A modeling study previously indicated that the cyclophilin, encoded by *S. aureus*, could be a single domain protein [42]. To confirm this proposition, we have individually performed limited proteolysis [51, 58-60, 62] of rCyp with trypsin, chymotrypsin, and proteinase K. Each of these enzymes is computationally determined to have higher than ten cleavage sites, which are distributed along the entire sequence of rCyp (Fig. 1A). This protein will mostly remain insensitive to the above enzymes if it is really composed of only one domain. We have noted the generation of primarily one proteolytic fragment from rCyp at the initial stage of its cleavage with proteinase K (Fig. 1B). One major fragment was also made at the early period of digestion of rCyp with trypsin (Fig. 1C) or chymotrypsin (Fig. 1D). The proteinase K-, trypsin- and chymotrypsin-generated fragments are designated as fragment I, fragment II and fragment III, respectively. All of the fragments remained stable during the entire period of digestion. The intensities of the fragments were gradually increased with the increase of time of digestion. Their molecular masses are about ~2-3 kDa less than that of rCyp, indicating that the digestion occurred at one end or both ends of this protein in the presence of proteinase K. Conversely, fragment II was possibly originated due to the removal of any one end of rCyp. On the other hand, fragment III might have been generated due to the cleavage of the less chymotrypsin-sensitive peptide bonds formed by Leu, Met, and His residues (web.expasy.org/peptide_cutter) at the end(s) of rCyp. Our Western blot analyses show

bioRxiv preprint doi: https://doi.org/10.1101/511048; this version posted January 3, 2019. The copyright holder for this preprint (which was not certified by peer review) is the author/funder, who has granted bioRxiv a license to display the preprint in perpetuity. It is made available under aCC-BY 4.0 International license.

223 no interaction between the proteolytic fragments and anti-His antibody (Figs. 1E-1G),
224 indicating the loss of polyhistidine tag from the N-terminal end of rCyp in the presence of
225 the above enzymes.
226
227 **Fig. 1. Characterization of rCyP by limited proteolysis.** (A) The amino acid sequence
228 of rCyp with the cut sites of chymotrypsin (Ch), trypsin (Tr), and proteinase K (Pr). The
229 predicted cleavage sites, found out by a software tool [58], are shown at the top and
230 bottom of the sequence using vertical lines. The polyhistidine tag of rCyp is composed of
231 residues 1-23. The rCyp fragments, generated from the partial digestion of rCyp with the
232 either of Pr (B), Tr (C), and Ch (D), were separated by different SDS-13.5% PAGE.
233 Arrowhead and I-III represent the intact rCyp and the major rCyp fragments,
234 respectively. (E, F, G) Western blotting experiment. The Pr-, Tr-, and Ch-generated rCyp
235 fragments were analyzed using an anti-his antibody. We have mentioned the mass of each
236 marker protein at the right-hand sides of the blot and gel images.
237
238 To find out the cut sites in rCyp, the masses of the above proteolytic fragments (I-
239 III) were estimated using a MALDI-TOF mass spectrometry as described [59]. The m/z
240 spectrum shows that there was a generation of two major peaks from rCyp digested with
241 proteinase K (S1A Fig.). Conversely, trypsin (S1B Fig.)- or chymotrypsin (S1C Fig.)-
242 digested rCyp resulted in largely one major peak as expected. As the two peaks obtained
243 from the proteinase K-digested rCyp were fused with each other, the fragment I might be
244 composed of two proteolytic fragments (designated as Ia and Ib) having a little difference
245 in molecular mass. The single major peak originated from the trypsin-digested rCyp most

bioRxiv preprint doi: https://doi.org/10.1101/511048; this version posted January 3, 2019. The copyright holder for this preprint (which was not certified by peer review) is the author/funder, who has granted bioRxiv a license to display the preprint in perpetuity. It is made available under aCC-BY 4.0 International license.

246 possibly corresponds to fragment II. Similarly, the peak yielded from the chymotrypsin-
247 cleaved rCyp might be due to fragment III. The molecular masses of the above rCyp
248 fragments, calculated using the m/z spectral data (S1 Fig.), were found to vary from
249 21493.63 to 22050.73 Da (Table 1). Using the predicted cut site data of rCyp (Fig. 1A),
250 different proteolytic fragments were generated followed by the determination of their
251 masses using a computational tool (web.expasy.org/protparam). The rCyp fragments
252 whose theoretical masses nearly matched with the experimental masses of fragments Ia,
253 Ib, II, and III are composed of the amino acid residues Ser 23 to Val 218, Ser 23 to Glu
254 219, Gly 18 to Glu 220, and Ala 22 to Glu 220, respectively (Fig. 1A). Thus, five peptide
255 bonds, made by the rCyp residues Arg 17 and Gly 18, Met 21 and Ala 22, Ala 22 and Ser
256 23, Val 218 and Glu 219, and Glu 219 and Glu 220, showed sensitivity to the proteolytic
257 enzymes employed in the investigation. Of the susceptible peptide bonds, three bonds are
258 in the polyhistidine tag carrying region of rCyp and the rest bonds are in the extreme C-
259 terminal end of this enzyme (Fig. 1A). Collectively, both ends of rCyp might be exposed
260 to its surface.

261

262 **Table 1. Mass and composition of the proteolytic fragments.**

Enzyme	rCyp fragments	Mass of rCyp fragments[A] (Da)	Composion of rCyp fragments[B]
Proteinase K	Ia	21493.63	Ser23-Val218
Proteinase K	Ib	21564.43	Ser23-Glu219
Trypsin	II	22050.73	Gly18-Glu220
Chymotrypsin	III	21973.69	Ala22-Glu220

263

264 [A]The masses of the rCyp fragments were estimated using MALDI-TOF data (S1 Fig.).
265 [B]The masses of fragments with the designated residue carrying regions, calculated by a

bioRxiv preprint doi: https://doi.org/10.1101/511048; this version posted January 3, 2019. The copyright holder for this preprint (which was not certified by peer review) is the author/funder, who has granted bioRxiv a license to display the preprint in perpetuity. It is made available under aCC-BY 4.0 International license.

266 computational tool (web.expasy.org/protparam), are very close to those determined using
267 MALDI-TOF data.
268
269 ## Unfolding of proteins
270 The unfolding pathways of many proteins appeared dissimilar in the presence of
271 different denaturants [49-51, 63]. Previously, both rCyp and rCyp-CsA in the presence of
272 GdnCl were unfolded via the production of one intermediate [42]. To check whether the
273 urea-induced unfolding of these proteins would follow the similar pathway, their far-UV
274 CD, intrinsic Trp fluorescence, and ANS fluorescence spectra were separately recorded
275 in the presence of 0 to 7/8 M urea (S2 Fig.) A monophasic curve is obtained for rCyp
276 when the ellipticity values at 222 nm were plotted against the matching urea
277 concentrations. Conversely, such a curve generated for rCyp-CsA was biphasic in nature
278 (Fig. 2A). A monophasic curve for rCyp and a biphasic curve for rCyp-CsA were also
279 obtained when we plotted their Trp fluorescence intensity (Fig. 2B) or the associated λ_{max}
280 (Fig. 2C) values against the related urea concentrations. The λ_{max} values of both proteins
281 were shifted to 350 nm when there was a saturation of fluorescence intensity. All of the
282 biphasic curves show the transitions at ~1.5/2 - 2.75/3 M and ~5/5.5 – 7/7.5 M urea,
283 respectively. Unlike the curves obtained using the CD and Trp fluorescence data, the
284 curves, prepared using the ANS fluorescence intensity values of rCyp and rCyp-CsA,
285 look very similar and possibly carry two transitions (Fig. 2D).
286
287 **Fig. 2. Unfolding studied by spectroscopic tools.** (A) The ellipticity values of rCyp and
288 rCyp-CsA at 222 nm, extracted from their far-UV CD spectra (S2 Fig.), were normalized

bioRxiv preprint doi: https://doi.org/10.1101/511048; this version posted January 3, 2019. The copyright holder for this preprint (which was not certified by peer review) is the author/funder, who has granted bioRxiv a license to display the preprint in perpetuity. It is made available under aCC-BY 4.0 International license.

289 and plotted against the corresponding urea concentrations as described [51]. (B) The
290 intrinsic Trp fluorescence intensity values of rCyp (at 343 nm) and rCyp-CsA (at 341
291 nm), obtained from the respective spectra (S2 Fig.), were normalized and plotted as
292 above. (C) The λ_{max} values of rCyp and rCyp-CsA, derived from the Trp fluorescence
293 spectra (S2 Fig.), were similarly plotted. (D) The ANS fluorescence intensity values of
294 rCyp, and rCyp-CsA at 480 nm, collected from the related spectra (S2 Fig.), were
295 identically normalized and plotted. All lines through the spectroscopic signals denote the
296 best-fit lines.
297
298 To verify the above unfolding data, we have also investigated the unfolding of
299 rCyp and rCyp-CsA using transverse urea gradient gel electrophoresis [51], a
300 biochemical probe. The migration of rCyp or rCyp-CsA across the urea gradient gel
301 yielded an S-shaped protein band having nearly a clear transition region (Fig. 3). The
302 rCyp-specific protein band shows a transition at ~3.25-4.25 M urea, whereas, that of
303 rCyp-CsA results in a transition region at ~4.75-5.75 M urea, indicating that the initiation
304 of the unfolding of drug-bound rCyp occurred at higher urea concentration. The faded
305 transition region also suggests a slow unfolding reaction [59, 61].
306
307 **Fig. 3. Transverse urea gradient polyacrylamide gel electrophoresis of proteins.**
308 Both rCyp and rCyp-CsA were separately analyzed by the Transverse urea gradient
309 polyacrylamide gel electrophoresis as described [51, 59].
310

bioRxiv preprint doi: https://doi.org/10.1101/511048; this version posted January 3, 2019. The copyright holder for this preprint (which was not certified by peer review) is the author/funder, who has granted bioRxiv a license to display the preprint in perpetuity. It is made available under aCC-BY 4.0 International license.

311 The reversibility of the unfolding reaction was checked by recording the Trp
312 fluorescence spectra of the native, denatured, and the probable refolded forms of rCyp
313 and rCyp-CsA as described [42]. We have observed that the Trp fluorescence spectra of
314 the native protein and the related refolded protein have completely coincided with each
315 other (Fig. 4A). Additional RNase T1 refolding assay reveals that there is nearly a
316 complete restoration of the PPIase activity in the renatured rCyp (Fig. 4B). In sum, both
317 rCyp and rCyp-CsA were unfolded by a reversible pathway in the presence of urea.
318
319 **Fig. 4. Refolding of the urea-exposed proteins.** (A) The intrinsic Trp fluorescence
320 spectra of the unfolded, native, and refolded rCyp or rCyp-CsA. (B) RNase T1 activity of
321 refolded and native rCyp.
322
323 ## Unfolding mechanism of the protein
324 To accurately determine the mechanism of the urea-induced unfolding of rCyp
325 and rCyp-CsA, all of the unfolding curves were examined using different models [24, 25,
326 58]. Each rCyp-specific curve, generated using CD or Trp fluorescence signals, exhibited
327 the best fitting with a two-state model [24]. The C_m values, obtained from the fitted CD
328 (Fig. 2A), Trp fluorescence intensity (Fig. 2B) and the λ_{max} (Fig. 2C) data of rCyp, are
329 3.82±0.04 M, 2.91 ± 0.07 M, and 3.30±0.06 M urea, respectively. Conversely, the rCyp-
330 specific curve, produced using ANS fluorescence signals, fit best to the three-state model
331 [25] with the resulted C_m values of ~1.18 M and ~3.68 M urea (Table 2). Thus, the ANS
332 fluorescence data suggest the formation of a rCyp intermediate at ~3 M urea (Fig. 5).
333 Two additional pieces of evidence have supported the above proposal. The fractions of

bioRxiv preprint doi: https://doi.org/10.1101/511048; this version posted January 3, 2019. The copyright holder for this preprint (which was not certified by peer review) is the author/funder, who has granted bioRxiv a license to display the preprint in perpetuity. It is made available under aCC-BY 4.0 International license.

denatured rCyp molecules, estimated from both the CD (Fig. 2A) and Trp fluorescence data (Fig. 2B), were plotted against 0-7 M urea and the resulted curves did not coincide with each other (S3A Fig.). The non-overlapping of such curves indicates the formation of unfolding intermediate [25]. Secondly, the phase diagram [29, 64], used to know about the formation of the hidden unfolding intermediate of proteins, was developed by plotting the Trp fluorescence intensities of rCyp at 320 nm against its fluorescence intensities at 365 nm (S3B Fig.). The yielded non-linear plot again suggests the formation of rCyp intermediate(s) at 0-7 M urea.

Table 2. Thermodynamic parameters of protein unfolding.

Protein	Assay method	Fitted equation	C_m (M)	m (kcal $mol^{-1}M^{-1}$)	ΔG^W (kcal M^{-1})	$\Delta\Delta G$ (kcal M^{-1})
rCyp	ANS fluorescence	Three-state	1.18±0.03 3.68±0.19	1.69±0.01 0.74±0.02	1.99±0.03 2.74±0.07	
	TUGE	Two-state	3.79±0.36	1.81±0.21	6.83±0.15	
rCyp-CsA	ANS fluorescence	Three-state	1.51±0.02 4.61±0.21	1.33±0.03 1.70±0.19	2.01±0.12 7.82±0.53	0.55±0.10 1.12±0.08
	TUGE	Two-state	5.53±0.56	1.44±0.19	7.92±0.27	2.81±0.02

The thermodynamic parameters were estimated from ANS fluorescence (Fig. 2D) and TUGE (Fig. 3) data using standard equations [24, 25].

Fig. 5. A graphic presentation of the urea-induced unfolding of rCyp and rCyp-CsA. The unfolding intermediates are denoted by rCyp' and rCyp-CsA'.

All of the unfolding data of rCyp-CsA (Fig. 2), accumulated from our spectroscopic studies, fit best to a three-state model, clearly suggesting the formation of a rCyp-CsA intermediate in the presence of urea. While the C_m values yielded from the

bioRxiv preprint doi: https://doi.org/10.1101/511048; this version posted January 3, 2019. The copyright holder for this preprint (which was not certified by peer review) is the author/funder, who has granted bioRxiv a license to display the preprint in perpetuity. It is made available under aCC-BY 4.0 International license.

353 CD data of rCyp-CsA are 2.09±0.22 M and 6.37±0.09 M, those from its Trp fluorescence
354 data are 2.58±0.17 and 6.5±0.05 M urea. Conversely, the C_m values estimated from the
355 ANS fluorescence signals of rCyp-CsA are ~1.51 M and ~4.61 M urea, respectively.
356 Jointly, a rCyp-CsA intermediate might have been generated at ~3-5 M urea (Fig. 5).

357 ## Stability of the protein

358 A protein is usually stabilized when it binds a ligand [28, 29, 33, 36, 37, 39, 42].
359 To see whether the stability of rCyp is increased in the presence of CsA, the C_m, m, ΔG^W,
360 and $\Delta\Delta G$ values (Table 2), obtained from the ANS fluorescence data of rCyp and rCyp-
361 CsA (Fig. 2D), were further analyzed as state above. The data show that the C_m values of
362 rCyp-CsA are significantly higher than those of rCyp (all p values <0.05). The difference
363 of free energy change between rCyp and rCyp-CsA (i.e. $\Delta\Delta G$) is more than ~0.5 kcal M^{-1}
364 (Table 2). The thermodynamic parameters, determined by fitting the TUGE data (Fig. 3)
365 with the two-state equation [24], are also presented in Table 2. The yielded ΔG^W and C_m,
366 values of rCyp-CsA were noted to be significantly higher than those of rCyp (all p values
367 ≈ 0.03). The free energy change $\Delta\Delta G$ between rCyp and rCyp-CsA is about 2.8 kcal M^{-1}
368 (Table 2). Taken together, we suggest that the stability of rCyp is increased in the
369 presence of CsA.

370 ## Properties of unfolding intermediates

371 To confirm the generation of unfolding intermediates, the urea-exposed rCyp and
372 rCyp-CsA were separately digested with trypsin as stated [58]. The yielded proteolytic
373 patterns of proteins at ~0-1 M urea look different from those in the presence ~2-6 M urea
374 (Fig. 6A). While new proteolytic fragments from rCyp appeared at ~3-6 M urea, those
375 from rCyp-CsA are generated at ~2-6 M urea. The emergence of the additional

bioRxiv preprint doi: https://doi.org/10.1101/511048; this version posted January 3, 2019. The copyright holder for this preprint (which was not certified by peer review) is the author/funder, who has granted bioRxiv a license to display the preprint in perpetuity. It is made available under aCC-BY 4.0 International license.

proteolytic fragments might be due to the change of protein structure at the above urea concentrations. Thus, the data prove the production of unfolding intermediates from both proteins at moderately higher urea concentrations.

Fig. 6. Properties of urea-made intermediates. (A) Analyses of the trypsin-generated fragments from rCyp and rCyp-CsA. Proteins were exposed to 0-7 M urea followed by their digestion with (+)/without (-) trypsin for 10 min at 25°C. All of the proteolytic fragments are resolved by SDS-13.5% PAGE. Arrowheads denote new protein fragments. (B) The near-UV CD spectra of rCyp and rCyp-CsA at the denoted concentrations of urea. The spectra were recorded using same concentrations of proteins. (C) Drug binding assay. The curves show the change of Trp fluorescence intensity of 0 M and 3 M urea-exposed rCyp (2 μM) in the presence of 0-3.5 μM Cyclosporin A (CsA).

The ellipticity value of rCyp at 222 nm was reduced about 4% when we enhanced the urea concentration from 0 M to 3 M urea (S4A Fig.), whereas, that of rCyp-CsA was dropped about 17% upon increasing the urea concentration from 0 M to 4 M urea. Therefore, both rCyp and rCyp-CsA intermediates are composed of sufficient extents of secondary structures.

The Trp fluorescence intensity of rCyp was decreased about 40% upon augmenting the urea concentrations from 0 M to 3 M (S4B Fig.). Conversely, there was a ~13% reduction of the Trp fluorescence intensity of rCyp-CsA when the urea concentration was enhanced from 0 M to 4 M. At the intermediate forming urea concentrations, the spectra of rCyp and rCyp-CsA are associated with the 4 nm and 2 nm

bioRxiv preprint doi: https://doi.org/10.1101/511048; this version posted January 3, 2019. The copyright holder for this preprint (which was not certified by peer review) is the author/funder, who has granted bioRxiv a license to display the preprint in perpetuity. It is made available under aCC-BY 4.0 International license.

399 red-shifted emission maxima, respectively. In sum, the tertiary structures of rCyp and
400 rCyp-CsA intermediates are different from those of the native forms of these proteins.

401 The ANS fluorescence intensities of rCyp at 3 M and rCyp-CsA at 4 M urea,
402 unlike their far-UV CD and Trp fluorescence intensities, are more than 70% less in
403 comparison with those of the related proteins at 0 M urea (S4C Fig.). Therefore, the
404 extent of the hydrophobic surface area in either intermediate is significantly less than that
405 in the related native protein.

406 The near-UV CD values of rCyp at ~280-285 nm were slightly decreased when
407 urea concentrations were augmented from 0 M to 3 M urea (Fig. 6B). On the contrary,
408 the near-UV CD values of rCyp-CsA at ~280-285 nm were marginally reduced upon
409 raising the urea concentrations from 0 M to 4 M. Collectively, both intermediates are not
410 molten globules [55] as they retained sufficient extent of tertiary structures.

411 To verify whether rCyp intermediate is biologically active, we estimated the Trp
412 fluorescence change of both 0 M and 3 M urea-equilibrated rCyp in the presence of
413 different concentrations of CsA (Fig. 6C). The yielded K_d values for the rCyp and CsA
414 interaction at 0 M and 3 M urea are 1.25 ±0.02 μM and 1.16±0.07 μM, respectively.
415 Further analysis reveals no significant change of K_d value (p=0.16) upon changing the
416 urea concentrations from 0 M to 3 M, indicating that rCyp intermediate did not lose any
417 drug binding activity.

418 ## Discussion

419 The present study has provided some seminal clues about the folding-unfolding
420 mechanism and the domain structure of rCyp, a chimeric SaCyp harboring 220 amino
421 acid residues [42]. Our limited proteolysis (Fig. 1) and the subsequent analyses (Table 1)

bioRxiv preprint doi: https://doi.org/10.1101/511048; this version posted January 3, 2019. The copyright holder for this preprint (which was not certified by peer review) is the author/funder, who has granted bioRxiv a license to display the preprint in perpetuity. It is made available under aCC-BY 4.0 International license.

have revealed that two rCyp ends carrying residues 1 to 22 and 218 to 220 are only susceptible to three proteolytic enzymes employed in the study. The rCyp region having residues 23 to 218 carries most of the cleavage sites of these enzymes (Fig. 1A). The absence of digestion in the internal rCyp region indicates the formation of a domain by the residues 23 to 218. Thus, the single domain structure of SaCyp proposed before on the basis of a modeling study data [42] was confirmed by our proteolysis results. However, such single domain structure is not unprecedented as the cyclophilins those have masses nearly similar to that of SaCyp are also shown to carry single domain capable of binding both the substrate and inhibitor [2, 3, 11, 19].

The proteolysis of Val 218 - Glu 219, and Glu 219 - Glu 220 peptide bonds (Fig. 1) indicates that the rCyp residues Val 218, Glu 219, and Glu 220, corresponding to SaCyp residues Val 195, Glu 196, and Glu 197, might be exposed to its surface. Our computational examination of the model SaCyp structure [42] reveals that four C-terminal end residues, Asp 194, Val 195, Glu 196 and Glu 197, are not involved in the formation of any secondary structure and more than 20% exposed to its surface (data not shown). We have noted that the extreme C-terminal end of some SaCyp homologs, formed by three to four residues, are also not structured but adequately surface-exposed. The above data not only support our proteolysis data but also indicate that a short flexible region is attached to the C-terminal end of SaCyp domain. Thus far, no other single domain cyclophilin was reported to carry a short tail at the C-terminal end.

Our spectroscopic data have indicated that unfolding of rCyp or rCyp-CsA at 0-7/8 M urea proceeds via the synthesis of one stable intermediate (Fig. 5). The unfolding pathway of either protein in the presence of urea was fully reversible though there was

bioRxiv preprint doi: https://doi.org/10.1101/511048; this version posted January 3, 2019. The copyright holder for this preprint (which was not certified by peer review) is the author/funder, who has granted bioRxiv a license to display the preprint in perpetuity. It is made available under aCC-BY 4.0 International license.

445 the production of an intermediate (Fig. 4). The surface hydrophobicity, secondary
446 structure, and the tertiary structure rCyp intermediate are not fully identical to those of
447 rCyp-CsA intermediate (Fig. 6 and S4 Fig.). The structural properties of the intermediates
448 also do not match with those of native proteins. Of the intermediates, the rCyp
449 intermediate is formed at comparatively less concentration of urea (Fig. 5). Collectively,
450 the number and type of non-covalent interactions responsible for stabilization of a protein
451 structure [68, 69] are possibly not identical in the two intermediates.

452 The unfolding mechanism of rCyp and rCyp-CsA in the presence of urea (Fig. 5)
453 matches with that of these proteins in the presence of GdnCl [42]. However, the GdnCl
454 concentration needed to make the rCyp intermediate was higher than that required to
455 synthesize rCyp-CsA intermediate. The structural properties of the urea-made
456 intermediates are also not completely identical to those of the GdnCl-generated
457 intermediates (Fig. 6). The GdnCl-made rCyp intermediate, unlike the urea-produced
458 rCyp intermediate (Fig. 6B), has a little extent of tertiary structure (S5A Fig.). On the
459 other hand, the GdnCl-made rCyp-CsA intermediate, like the urea-created rCyp-CsA
460 intermediate, has retained some tertiary structure (S5A Fig.) but lost most of the
461 hydrophobic surface area (S5B Fig.). In sum, neither the GdnCl-generated nor the urea-
462 made intermediates have the properties of a molten globule [55].

463 The unfolding mechanism of drug-bound/unbound rCyp shows some similarity
464 and dissimilarity with those of other drug-bound/unbound cyclophilins [40, 41, 43]. A
465 yeast-encoded cyclophilin (CPR3) in the presence of urea was unfolded by means of the
466 creation of two structurally different intermediates [43]. Of the CPR3 intermediates, the
467 intermediate formed at relatively less urea concentration has the characteristics of a

bioRxiv preprint doi: https://doi.org/10.1101/511048; this version posted January 3, 2019. The copyright holder for this preprint (which was not certified by peer review) is the author/funder, who has granted bioRxiv a license to display the preprint in perpetuity. It is made available under aCC-BY 4.0 International license.

468 molten globule [55]. Like rCyp, LdCyp, a cyclophilin synthesized by *Leishmania*
469 *donovani* [41], was unfolded by a three-state mechanism in the presence of GdnCl.
470 However, the LdCyp intermediate, unlike rCyp intermediate, has the properties of a
471 molten globule [55]. On the other hand, the urea-induced unfolding of a mycobacterial
472 cyclophilin (PpiA) or its drug-bound form occurred via the formation of an intermediate
473 [40]. Currently, little is known about the biological activities of CPR3, LdCyp, and PpiA
474 intermediates. Conversely, our studies for the first time have indicated that the drug
475 binding activities of the urea-made rCyp intermediate and native rCyp are nearly similar
476 (Fig. 6C). The GdnCl-made rCyp intermediate also retained about 25% of the total drug
477 binding activity of native rCyp (S5 Fig.).

478 The complete retention of drug binding activity in the rCyp intermediate (Fig. 6C)
479 implies no significant alteration of the three-dimensional structure of the cyclosporin A
480 binding site in the presence of 3 M urea. Our previous studies showed that the putative
481 cyclosporin A binding site in SaCyp is primarily located in the regions harboring residues
482 ~Arg 59 to Phe 116 and ~Trp 152 to His 157 [42]. Therefore, the structural change noted
483 in rCyp intermediate (Fig. 2) possibly have occurred at regions carrying residues ~Ala 2
484 to His 58, ~Ile 117 to Pro 151, and ~Thr 158 to Glu 197. Besides Trp 152, SaCyp carries
485 another Trp residue at position 136 [42]. The former Trp residue is relatively more
486 exposed on the surface of SaCyp (data not shown). As Trp 152 is conserved and
487 indispensable for binding CsA [1], there might be little change of the structure around
488 this residue in the rCyp intermediate. The altered Trp fluorescence intensity and emission
489 maxima of the rCyp intermediate (Figs. 2B and 2C), therefore, suggests a structural

bioRxiv preprint doi: https://doi.org/10.1101/511048; this version posted January 3, 2019. The copyright holder for this preprint (which was not certified by peer review) is the author/funder, who has granted bioRxiv a license to display the preprint in perpetuity. It is made available under aCC-BY 4.0 International license.

change around Trp 136. Additional studies are needed to prove the urea-induced structural alteration around Trp 136 with certainty.

Many promising CsA analogs with no immunosuppressive activity were discovered and suggested to be useful in treating various diseases [2, 16-18, 70]. As these analogs did not yield encouraging results in the clinical trials [10, 11], screening or synthesis of additional CsA analogs should be continued on a priority basis. An inhibitor can be easily screened against a drug target if the binding of the former increases the midpoint of unfolding transition (or the stability) of the latter [33-39]. Several chemical denaturation-based assay systems were reported to screen the drug molecules against various drug targets including PPIase enzymes [28, 34, 35, 37, 39]. Our present (Table 2) and previous [42] unfolding results demonstrated the significant increment of the stability of rCyp in the presence of CsA. The urea-induced unfolding of a mycobacterial cyclophilin also reported its stabilization by CsA [40]. Collectively, an unfolding-based assay system could be developed using SaCyp or rCyp for screening new CsA analogs in the future.

Conclusions

Our investigations have provided invaluable clues about the basic structure and the folding-unfolding mechanism of SaCyp, an *S. aureus*-encoded cyclophilin involved in pathogenesis. We noted that rCyp, a recombinant SaCyp, is a single-domain protein with a short tail at its C-terminal end. Additionally, rCyp unfolds via the formation of an intermediate in the presence of urea. The rCyp intermediate lacks the characteristics of a molten globule and also shows little loss of CsA binding activity. The unfolding of the

bioRxiv preprint doi: https://doi.org/10.1101/511048; this version posted January 3, 2019. The copyright holder for this preprint (which was not certified by peer review) is the author/funder, who has granted bioRxiv a license to display the preprint in perpetuity. It is made available under aCC-BY 4.0 International license.

512 CsA-bound rCyp also similarly occurred in the presence of urea. The stability data of
513 rCyp seems to be applicable in the discovery of new CsA derivatives in the future.

514 ## Acknowledgments

515 We thank Mr. S. Biswas, and Mr. M. Das for their excellent technical support.

516 ## References

517 1. Göthel SF, Marahiel MA. Peptidyl-prolyl cis-trans isomerases, a superfamily of
518 ubiquitous folding catalysts. Cell Mol Life Sci. 1999; 55: 423–436.
519 2. Nigro P, Pompilio G, Capogrossi MC.Cyclophilin A: a key player for human
520 disease. Cell Death Dis. 2013; 4: e888.
521 3. Ünal CM, Steinert M. Microbial Peptidyl-Prolyl *cis/trans* Isomerases (PPIases):
522 Virulence Factors and Potential Alternative Drug Targets. Microbiol Mol Biol
523 Rev. 2014; 78: 544-71.
524 4. Dimou M, Venieraki A, Katinakis P. Microbial Cyclophilins: specialized
525 functions in virulence and beyond. World J Microbiol Biotechnol. 2017; 33: 164.
526 5. Barik S. A Family of Novel Cyclophilins, Conserved in the Mimivirus Genus of
527 the Giant DNA Viruses.Comput Struct Biotechnol J. 2018; 16: 231-236.
528 6. Naoumov NV, Cyclophilin inhibition as potential therapy for liver diseases. J.
529 Hepatol. 2014; 61: 1166-1174.
530 7. Harikishore A, Yoon HS, Immunophilins: Structures, Mechanisms and Ligands.
531 Curr Mol Pharmacol. 2016; 9: 37-47.
532 8. Lavin PTM, McGee MM, Cyclophilin function in Cancer; lessons from virus
533 replication. Curr Mol Pharmacol. 2016; 9: 148-164.

bioRxiv preprint doi: https://doi.org/10.1101/511048; this version posted January 3, 2019. The copyright holder for this preprint (which was not certified by peer review) is the author/funder, who has granted bioRxiv a license to display the preprint in perpetuity. It is made available under aCC-BY 4.0 International license.

9. Dawar FU, Xiong Y, Khattak MNK, Li J, Lin L, Mei J, Potential role of cyclophilin A in regulating cytokine secretion. J. Leukoc. Biol. 2017; 102: 989-992.

10. Dunyak BM, Gestwicki JE, Peptidyl-Proline Isomerases (PPIases): Targets for Natural Products and Natural Product-Inspired Compounds. J. Med. Chem. 2016; 59: 9622-9644.

11. de Wilde AH, Zevenhoven-Dobbe JC, Beugeling C, Chatterji U, de Jong D, Gallay P, et al., Coronaviruses and arteriviruses display striking differences in their cyclophilin A-dependence during replication in cell culture. Virology 2018; 517: 148-156.

12. McCaffrey PG, Luo C, Kerppola TK, Jain J, Badalian TM, Ho AM, et al., Isolation of the Cyclosporin-Sensitive T Cell Transcription Factor NFATp. Science 1993; 262: 750-754.

13. Matsuda S, Koyasu S, Mechanisms of action of Cyclosporin, Immunopharmacology. 2000; 47:119-125.

14. Wang P, Heitman J, The cyclophilins. Genome Biol. 2005; 6: 226.

15. Naesens M, Kuypers DRJ, Sarwal M, Calcineurin Inhibitor Nephrotoxicity. Clin J Am SocNephrol. 2009; 4:481-508.

16. Quarato G, D'Aprile A, Gavillet B, Vuagniaux G, Moradpour D, Capitanio N, et al., The Cyclophilin Inhibitor Alisporivir Prevents Hepatitis C Virus-Mediated Mitochondrial Dysfunction. Hepatology. 2012; 55: 1333-1343.

17. Hopkins S, Gallay PA, The role of immunophilins in viral infection. Biochim. Biophys. Acta. 2015; 1850: 2103-2110.

bioRxiv preprint doi: https://doi.org/10.1101/511048; this version posted January 3, 2019. The copyright holder for this preprint (which was not certified by peer review) is the author/funder, who has granted bioRxiv a license to display the preprint in perpetuity. It is made available under aCC-BY 4.0 International license.

557 18. Kahlert V, Prell E, Ohlenschlager O, Melesina J, Schumann M, Lücke C, et al.,
558 Synthesis and biochemical evaluation of two novel N-hydroxy alkylated
559 cyclosporin A analogs. Org. Biomol. Chem. 2018; 16: 4338-4349.
560 19. Schiene-Fischer C. Peptidyl Prolyl *cis/trans* isomerases. In: Maccarrone M,
561 Valpuesta JM, editors. eLS Citable reviews in the Life Science.New Jersey:
562 John Wiley & Sons, Inc.; 2015.
563 20. Peterson MR, Hall DR, Berriman M, Nunes J, Leonard GA, Fairlamb AH, et
564 al., The three-dimensional structure of a *Plasmodium falciparum* cyclophilin in
565 complex with the potent anti-malarial Cyclosporin A. J. Mol. Biol. 2000; 298:
566 123-133.
567 21. Venugopal V, Datta AK, Bhattacharyya D, Dasgupta D, Banerjee R, Structure
568 of cyclophilin from *Leishmania donovani* bound to cyclosporin at 2.6 Å
569 resolution: correlation between structure and thermodynamic data. Acta Cryst.
570 D 2009; 65: 1187-1195.
571 22. Spitzfaden C, Weber HP, Braun W, Kallen J, Wider G, Widmer H, et al.,
572 Cyclosporin A-cyclophilin complex formation A model based on X-ray and
573 NMR data. FEBS Lett. 1992; 300: 291-300.
574 23. Kallen J, Spitzfaden C, Zurini MG, Wider G, Widmer H, Wüthrich K, et al.,
575 Structure of human cyclophlin and its binding site for Cyclosporin A
576 determined by X-ray crystallography and NMR spectroscopy. Nature 1991;
577 353: 276-279.
578 24. Pace CN, Shaw KL, Linear extrapolation method of analyzing solvent
579 denaturation curves. Proteins Suppl. 2000; 4: 1-7.

bioRxiv preprint doi: https://doi.org/10.1101/511048; this version posted January 3, 2019. The copyright holder for this preprint (which was not certified by peer review) is the author/funder, who has granted bioRxiv a license to display the preprint in perpetuity. It is made available under aCC-BY 4.0 International license.

580 25. Sancho J, The stability of 2-state, 3-state and more-state proteins from simple
581 spectroscopic techniques…plus the structure of the equilibrium intermediates at
582 the same time. Arch. Biochem. Biophys. 2013; 531: 4-13.
583 26. Connelly PR, Thomson JA, Heat capacity changes and hydrophobic interactions
584 in the binding of FK506 and rapamycin to the FK506 binding protein. Proc.
585 Natl. Acad. Sci. 1992; 89: 4781-4785.
586 27. Main ERG, Fulton KF, Jackson SE, Context-Dependent Nature Destabilizing
587 Mutations on the Stability of FKBP12. Biochemistry. 1998; 37: 6145-6153.
588 28. Gaudet M, Remtulla N, Jackson SE, Main ERG, Bracewell DG, Aeppli G, et
589 al., Protein denaturation and protein: drugs interactions from intrinsic protein
590 fluorescence measurements at the nanolitre scale. Protein Sci. 2010; 19: 1544-
591 1554.
592 29. Polley S, Jana B, Chakrabarti G, Sau S, Inhibitor-Induced Conformational
593 Stabilization and Structural Alteration of a Mip-Like Peptidyl Prolyl cis-trans
594 Isomerase and Its C-Terminal Domain. PLoS One. 9: e102891.
595 30. Polley S, Chakravarty D, Chakrabarti G, Chattopadhyaya R, Sau S, Proline
596 substitutions in a Mip-like peptidyl-prolyl cis-trans isomerase severely affect its
597 structure, stability, shape and activity. Biochimie Open. 2015; 1: 28-39.
598 31. Mahapa A, Mandal S, Sinha D, Sau S, Sau K, Determining the Roles of a
599 Conserved α-Helix in a Global Virulence Regulator from *Staphylococcus*
600 *aureus*. Protein J. 2018; 37: 103-112.
601 32. Mandal S, Ghosh S, Sinha D, Seal S, Mahapa A, Polley S, Saha D, Sau K,
602 Bagchi A, Sau S, Alanine substitution mutations in the DNA-binding region of

bioRxiv preprint doi: https://doi.org/10.1101/511048; this version posted January 3, 2019. The copyright holder for this preprint (which was not certified by peer review) is the author/funder, who has granted bioRxiv a license to display the preprint in perpetuity. It is made available under aCC-BY 4.0 International license.

603 a global staphylococcal virulence regulator affect its structure, function and
604 stability. Int. J. Biol. Macromol. 2018; 113: 1221-1232.
605 33. Waldron TT, Murphy KP, Stabilization of proteins by ligand binding:
606 application to drug screening and determination of unfolding energetic.
607 Biochemistry 2003; 42: 5058-5064.
608 34. Aucamp JP, Cosme AM, Lye GJ, Dalby PA, High-throughput measurement of
609 protein stability in microtiter plates. Biotechnol. Bioeng. 2005; 89: 599-607.
610 35. Aucamp JP, Martinez-Torres RJ, Hibbert EG, Dalby PA, A microplate-based
611 evaluation of complex denaturation pathways: structural stability of *Escherichia*
612 *coli* transketolase. Biotechnol. Bioeng. 2008; 99: 1303-10.
613 36. Cimmperman P, Baranauskiene L, Jachimoviciūte S, Jachno J, Torresan J,
614 Michailoviene V, et al., A quantitative model of thermal stabilization and
615 destabilization of proteins by ligands. Biophys. J. 2008; 95: 3222-31.
616 37. Mahendrarajah K, Dalby PA, Wilkinson B, Jackson SE, Main ER. A high-
617 throughput fluorescence chemical denaturation assay as a general screen for
618 protein-ligand binding. Anal. Biochem. 2011; 411: 155-157.
619 38. Senisterra G, Chau I, Vedadi M. Thermal Denaturation Assays in Chemical
620 Biology. Assay Drug Dev Technol. 2012; 10: 129-136.
621 39. Schön A, Brown RK, Hutchins BM, Freire E. Ligand binding analysis and
622 screening by chemical denaturation shift. Anal. Biochem. 2013; 443: 52-7.
623 40. Mitra D, Mukherjee S, Das AK.Cyclosporin A binding to *Mycobacterium*
624 *tuberculosis* peptidyl-prolyl cis-trans isomerase A- Investigation by CD, FTIR
625 and fluorescence spectroscopy. FEBS Lett. 2006; 580: 6846-6860.

bioRxiv preprint doi: https://doi.org/10.1101/511048; this version posted January 3, 2019. The copyright holder for this preprint (which was not certified by peer review) is the author/funder, who has granted bioRxiv a license to display the preprint in perpetuity. It is made available under aCC-BY 4.0 International license.

626 41. Roy S, Basu S, Datta AK, Bhattacharyya D, Banerjee R, Dasgupta D.
627 Equilibrium unfolding of cyclophilin from *Leishmania donovani*:
628 Characterization of intermediate states. Int. J. Biol. Macromol. 2014; 69: 353-
629 360.
630 42. Polley S, Seal S, Mahapa A, Jana B, Biswas A, Mandal S, et al., Identification
631 and characterization of a Cyclosporin binding cyclophilin from *Staphyococcus*
632 *aureus* Newman. Bioinformation. 2017; 13: 78-85.
633 43. Shukla VK, Singh JS, Vispute N, Ahmad B, Kumar A, Hosur RV. Unfolding of
634 CPR3 Gets Initiated at the Active Site and Proceeds via Two Intermediates.
635 Biophys. J. 2017; 112: 605-619.
636 44. Anderson KL, Roberts C, Disz T, Vonstein V, Hwang K, Overbeek R, et al.,
637 Characterization of the *Staphylococcus aureus* Heat Shock, Cold Shock,
638 Stringent and SOS responses and Their Effects on Log-Phase mRNA Turnover.
639 J. Bacteriol. 2006; 188: 6739-6756.
640 45. Zhang R, Lin Y. DEG5.0, a database of essential genes in both prokaryotes and
641 eukaryotes. Nucleic Acids Res. 2009; 37: 455-458.
642 46. Wiemels RE, Cech SM, Meyer NM, Burke CA, Weiss A, Parks AR, et al.. An
643 Intracellular Peptidyl-Prolyl cis/trans Isomerase Is Required for Folding and
644 Activity of the *Staphylococcus aureus* Seccreted Virulence Factor Nuclease. J.
645 Bacteriol. 2016; 199: e00453.
646 47. Keogh RE, Zapf RL, Wiemels RE, Wittekind MA, Carroll RK. The
647 intracellular cyclophilinPpiB contributes to the virulence of *Staphylococcus*
648 *aureus* independent of its PPIase activity. Infect Immun 2018; 86: e00379-18.

bioRxiv preprint doi: https://doi.org/10.1101/511048; this version posted January 3, 2019. The copyright holder for this preprint (which was not certified by peer review) is the author/funder, who has granted bioRxiv a license to display the preprint in perpetuity. It is made available under aCC-BY 4.0 International license.

649 48. Hiramatsu K, Katayama Y, Matsuo M, Sasaki T, Morimoto Y, Sekiguchi A, et
650 al., Multi-drug-resistant *Staphylococcus aureus* and future chemotherapy. J.
651 Infect. Chemother. 2014; 20: 593-601.
652 49. Assis LM, Nedeljković M, Dessen A. New strategies for targeting and
653 treatment of multi-drug resistant *Staphylococcus aureus*. Drug Resist. Updat.
654 2017; 31: 1-14.
655 50. Foster TJ. Antibiotic resistance in *Staphylococcus aureus*. Current status and
656 future prospects. FEMS Microbiol. Rev. 2017; 41: 430-449.
657 51. Akhtar MS, Ahmad A, Bhakuni V. Guanidinium Chloride- and Urea-Induced
658 Unfolding of the Dimeric Enzyme Glucose Oxidase. Biochemistry. 2002; 41:
659 3819-3827.
660 52. Rashid F, Sharma S, Bano B. Comparison of Guanidine Hydrochloride
661 (GdnHCl) and Urea Denaturation on Inactivation and Unfolding of Human
662 Placental Cystatin (HPC). Protein J. 2005; 24: 283-292.
663 53. Singh AR, Joshi S, Arya R, Kayastha AM, Saxena JK. Guanidine hydrochloride
664 and urea-induced unfolding of *Brugia malayi* hexokinase. Eur. Biophys. J.
665 2010; 39: 289-297.
666 54. Jana B, Bandhu A, Mondal R, Biswas A, Sau K, Sau S. Domain Structure and
667 Denaturation of a Dimeric Mip-like Peptidyl-Prolyl cis-trans Isomerase from
668 *Escherichia coli*. Biochemistry. 2012; 51: 1223-1237.
669 55. Arai M, Kuwajima K, Role of the molten globule state in protein folding.In:
670 Matthews CR, editors. Advances in Protein Chemistry.Cambridge: Academic
671 Press. Inc.; 2000, pp. 209-282.

bioRxiv preprint doi: https://doi.org/10.1101/511048; this version posted January 3, 2019. The copyright holder for this preprint (which was not certified by peer review) is the author/funder, who has granted bioRxiv a license to display the preprint in perpetuity. It is made available under aCC-BY 4.0 International license.

672 56. Sambrook J, Russell DW. Molecular Cloning: A Laboratory Manual. 3rd ed.
673 New York: Cold Spring Harbor Laboratory Press; 2001.
674 57. Ausubel FM. Current Protocols in Molecular Biology. New York: Greene Pub.
675 Associates and Wiley-Interscience; 1987.
676 58. Sinha D, Mondal R, Mahapa A, Sau K, Chattopadhyaya R, Sau S. A
677 staphylococcal anti-sigma factor possesses a single-domain, carries different
678 denaturant-sensitive regions and unfolds via two intermediates. PLoS One.
679 2018; 13: e0195416.
680 59. Mahapa A, Mandal S, Biswas A, Jana B, Polley S, Sau S, et al., Chemical and
681 thermal unfolding of a global staphylococcal virulence regulator with a flexible
682 C-terminal end. PLoS One. 2015; 10: e0122168.
683 60. Pal A, Chattopadhyaya R. Digestion of the λ cI Repressor with Various Serine
684 Proteases and Correlation with Its Three Dimensional Structure. J Biomol
685 Struct Dyn. 2008; 26: 339-353.
686 61. Goldenberg DP, Creighton TE. Gel Electrophoresis in Studies of Protein
687 Conformation and Folding. Anal. Biochem. 1984; 138: 1–18.
688 62. Fontana A, de Laureto PP, Spolaore B, Frare E, Picotti P, Zambonin M.
689 Probing protein structure with limited proteolysis. Acta Biochim. Pol. 2004; 51:
690 299-321.
691 63. Liu CP, Li ZY, Huang GC, Perrett S, Zhou JM. Two distinct intermediates of
692 trigger factor are populated during guanidine denaturation. Biochimie. 2005;
693 87: 1023-1031.

bioRxiv preprint doi: https://doi.org/10.1101/511048; this version posted January 3, 2019. The copyright holder for this preprint (which was not certified by peer review) is the author/funder, who has granted bioRxiv a license to display the preprint in perpetuity. It is made available under aCC-BY 4.0 International license.

64. Kuznetsova IM, Turoverov KK, Uversky VN. Use of the Phase Diagram Method to Analyze the Protein Unfolding-Refolding Reactions: Fishing Out the "Invisible" Intermediates. J. Proteome Res. 2004; 3: 485-494.

65. Ke H, Zhao Y, Luo F, Weissman I, Friedman J. Crystal structure of murine cyclophilin C complexed with immunosuppressive drug cyclosporin A. Proc Natl Acad Sci. 1993; 90: 11850-11854.

66. Davis TL, Walker JR, Campagna-Slater V, Finerty PJ, Paramanathan R, Bernstein G, et al., Structural and biochemical characterization of the human cyclophilin family of peptidyl-prolyl isomerases. PLoS Biol. 2010; 8: e1000439.

67. Mikol V, Kallen J, Walkinshaw MD. X-ray structure of a cyclophilin B/cyclosporin complex: comparison with cyclophilin A and delineation of its calcineurin-binding domain. Proc Natl Acad Sci. USA. 1994; 91: 5183-5186.

68. Pace CN, Shirley BA, McNutt M, Gajiwala K. Forces contributing to the conformational stability of proteins. FASEB J. 1996; 10: 75-83.

69. Jaenicke R. Stability and stabilization of globular proteins in solution. J. Biotechnol. 2000; 79: 193-203.

70. Zhao X, Xia C, Wang X, Wang H, Xin M, Yu L, Liang Y. Cyclophilin J PPIase Inhibitors Derived from 2,3-Quinoxaline-6 Amine Exhibit Antitumor Activity. Front Pharmacol. 2018; 9: 126.

Supporting Information

S1 Fig. Analysis of the proteolytic fragments by MALDI-TOF mass spectroscopy. The fragments resulted from the digestion of rCyp with proteinase K (A), trypsin (B), and

bioRxiv preprint doi: https://doi.org/10.1101/511048; this version posted January 3, 2019. The copyright holder for this preprint (which was not certified by peer review) is the author/funder, who has granted bioRxiv a license to display the preprint in perpetuity. It is made available under aCC-BY 4.0 International license.

717 chymotrypsin (C) were processed (as mentioned in Materials and methods) followed by
718 the recording of their spectra using a MALDI-TOF equipment. The 'm' and 'z' indicate
719 mass and charge number of ions, respectively.

720 **S2 Fig. Unfolding of proteins.** Far UV CD (A and B), intrinsic Trp fluorescence (C and
721 D), ANS fluorescence (E and F) of rCyp (A, C, and E) and rCyp-CsA (B, D, and F) in the
722 presence of denoted concentrations of urea.

723 **S3 Fig. Proof of unfolding rCyp intermediate.** (A) The fraction of unfolded rCyp
724 molecules, calculated using the θ_{222} (Fig. 2A) or Trp fluorescence intensity (Fig. 2B)
725 values and a standard equation [24], were plotted against 0-7 M urea. (B) Phase diagram
726 shows the unfolding of rCyp at 0-7 M urea. I_{320} and I_{365} indicate the Trp fluorescence
727 intensity values (extracted from S2C Fig.) of rCyp at 320 nm and at 365 nm, respectively.

728 **S4 Fig. Structure of urea-made intermediates.** The far-UV CD (A), intrinsic Trp
729 fluorescence (B), and ANS fluorescence (C) spectra of rCyp and rCyp-CsA at the
730 denoted concentrations of urea. The spectra at the indicated urea concentrations were
731 collected from S2 Fig.

732 **S5 Fig. Characteristics of intermediates made by GdnCl.** The near-UV CD (A) and
733 the ANS fluorescence (B) spectra of rCyp and rCyp-CsA at the shown GdnCl
734 concentrations. The spectra were recorded using equimolar concentrations of proteins.
735 The rCyp and rCyp-CsA intermediates were formed at 1.5 M and 0.6 M GdnCl,
736 respectively [42]. (C) CsA binding assay. The curve represents the alteration of Trp
737 fluorescence intensity of 1.5 M GdnCl-treated rCyp (2 μM) in the presence of 0-3.5 μM
738 CsA.

bioRxiv preprint doi: https://doi.org/10.1101/511048; this version posted January 3, 2019. The copyright holder for this preprint (which was not certified by peer review) is the author/funder, who has granted bioRxiv a license to display the preprint in perpetuity. It is made available under aCC-BY 4.0 International license.

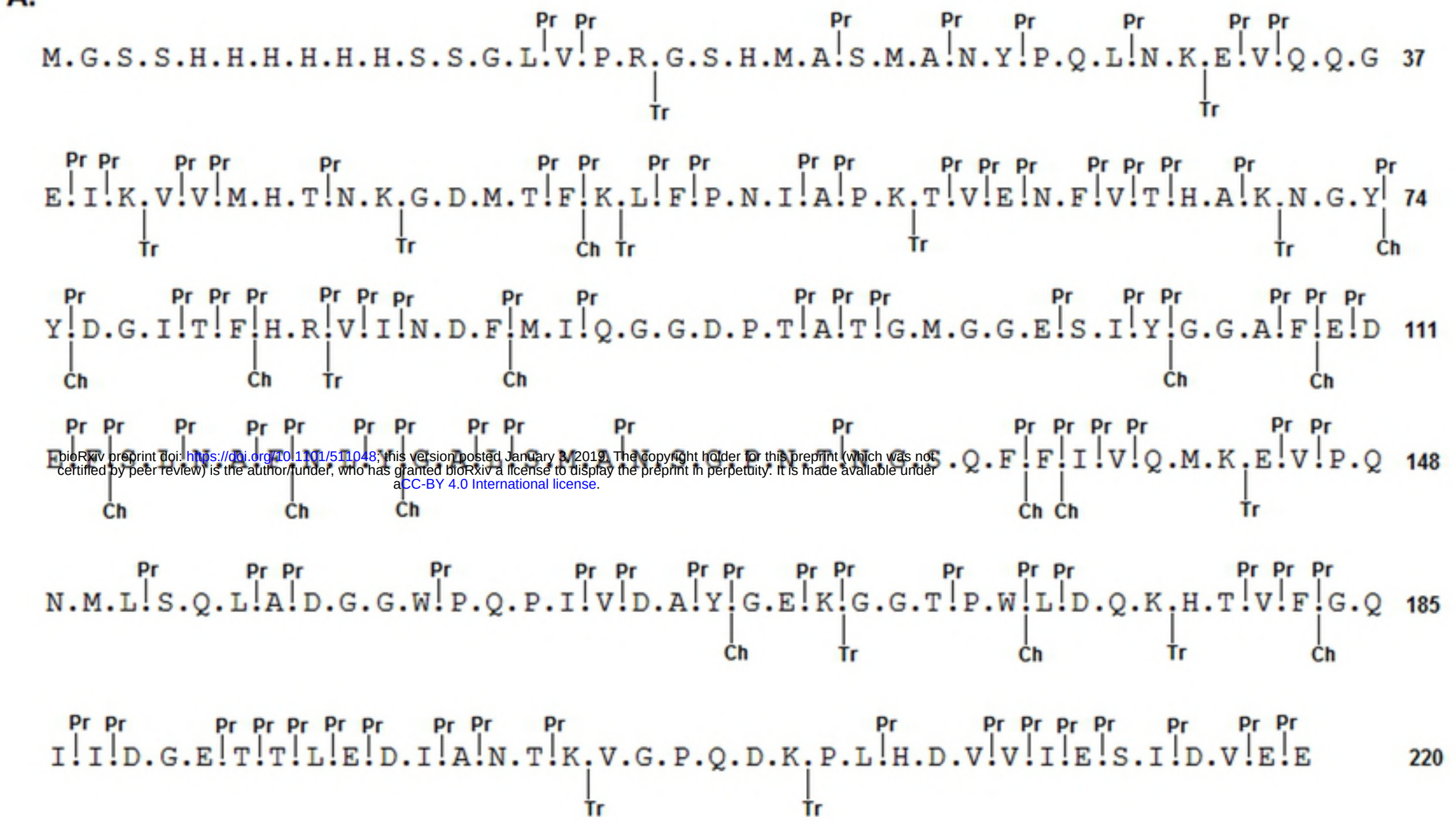

Figure 1

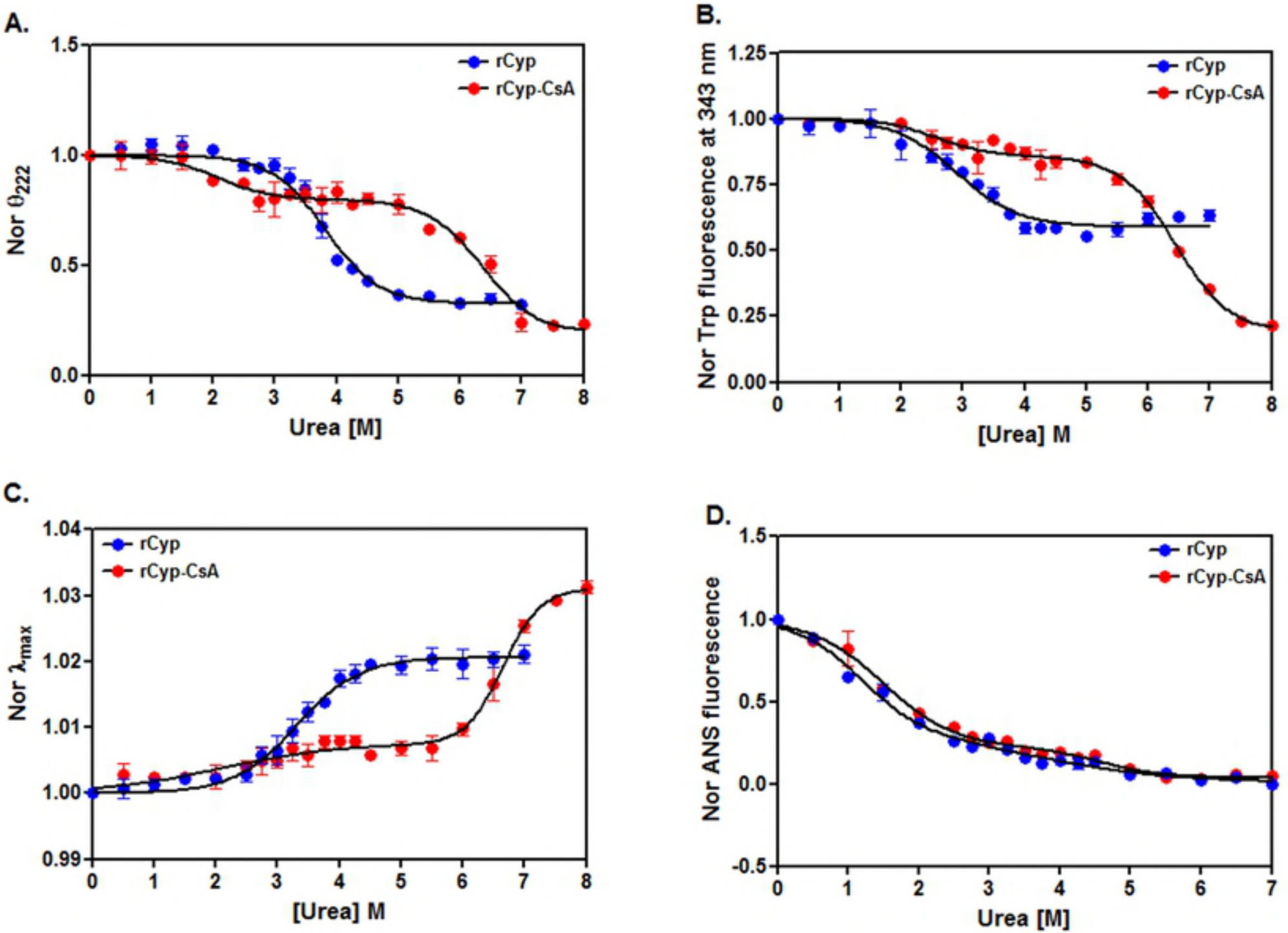
A.
Nor θ222
Urea [M]
rCyp
rCyp-CsA
B.
Nor Trp fluorescence at 343 nm
[Urea] M
rCyp
rCyp-CsA
C.
Nor λmax
[Urea] M
rCyp
rCyp-CsA
D.
Nor ANS fluorescence
Urea [M]
rCyp
rCyp-CsA

Figure 2

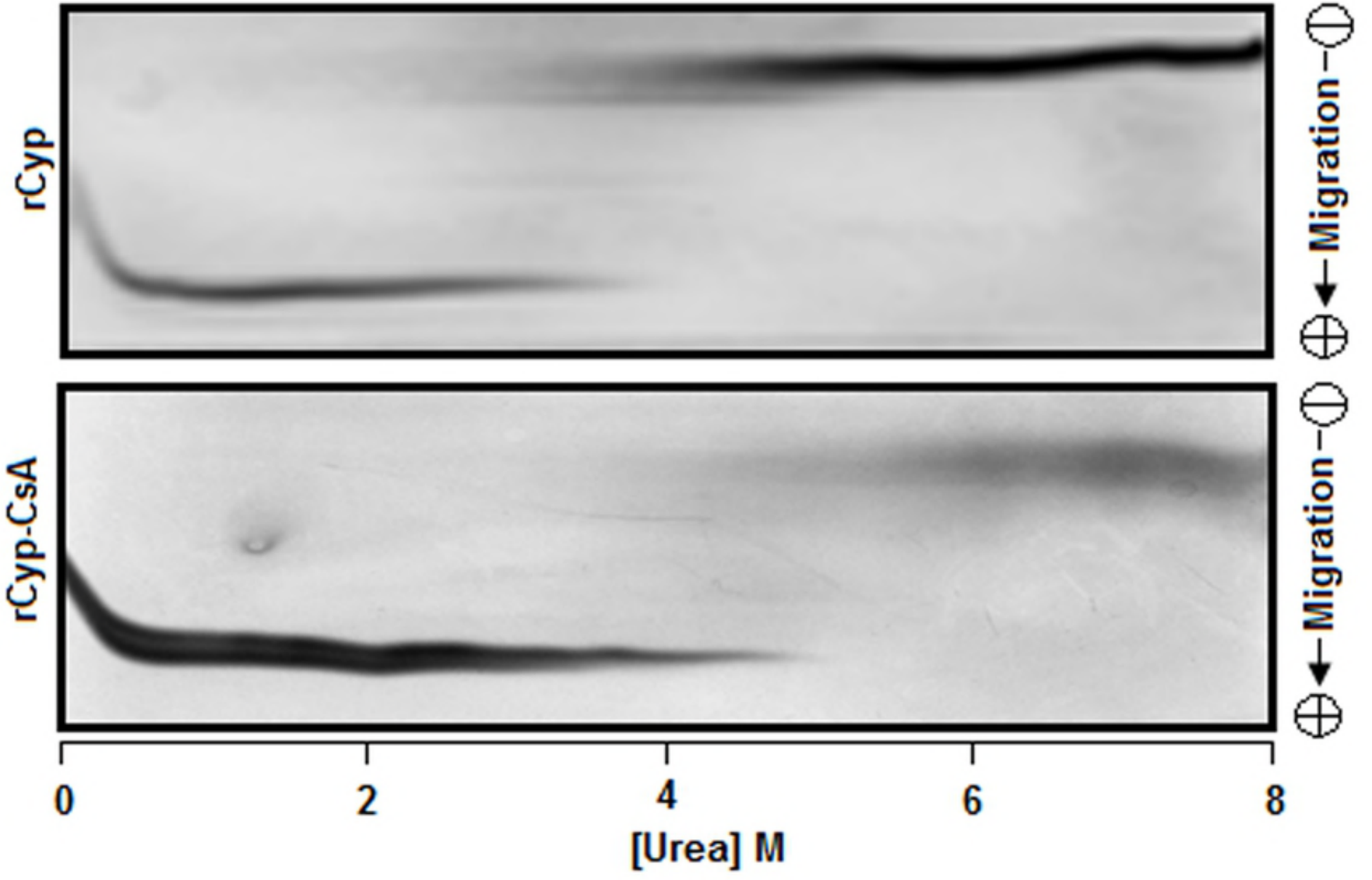

Figure 3

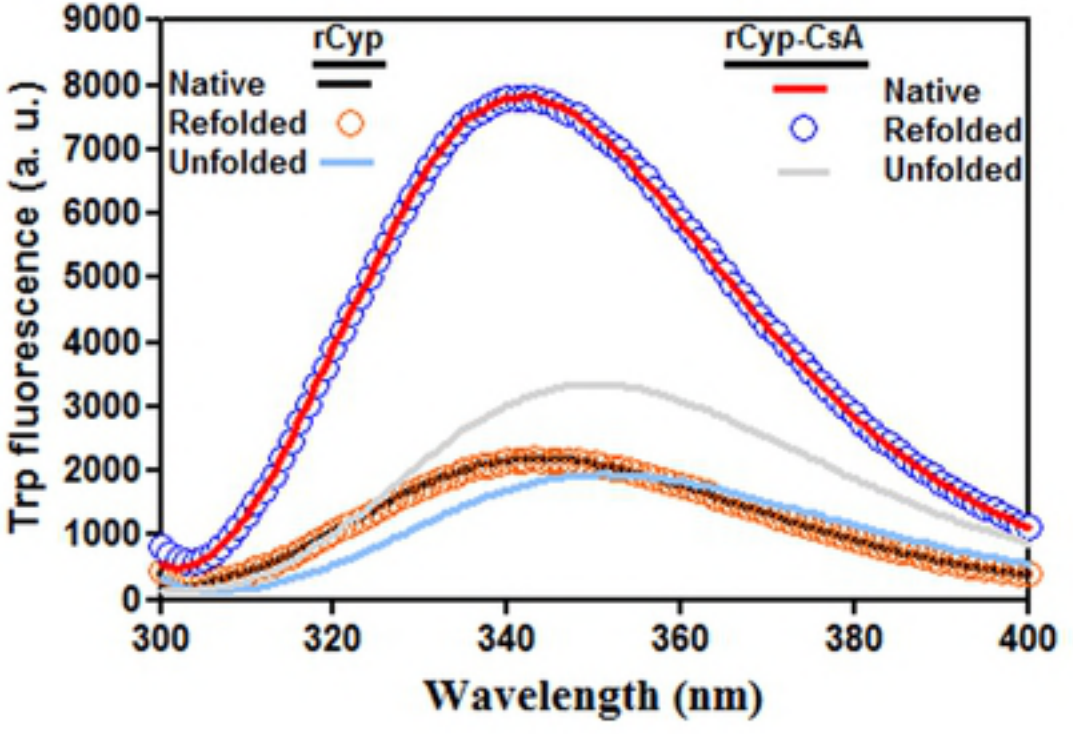
rCyp
rCyp-CsA
Native
Refolded
Unfolded
Native
Refolded
Unfolded
Trp fluorescence (a. u.)
Wavelength (nm)
9000
8000
7000
6000
5000
4000
3000
2000
1000
0
300
320
340
360
380
400

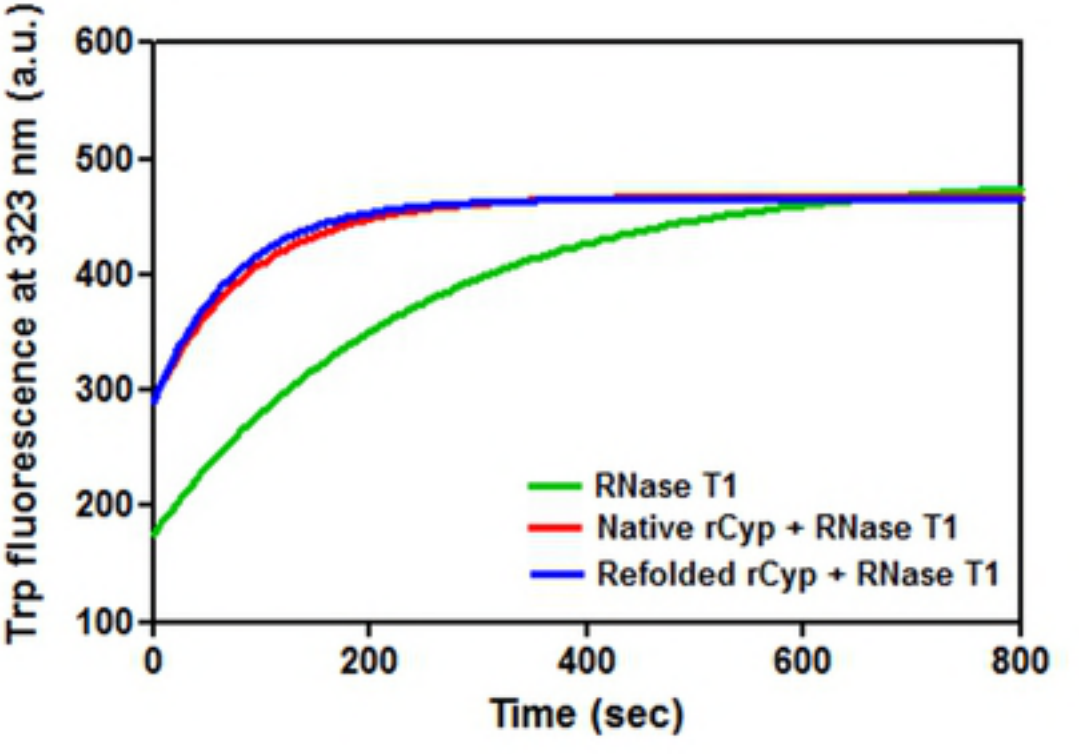
Trp fluorescence at 323 nm (a.u.)
Time (sec)
RNase T1
Native rCyp + RNase T1
Refolded rCyp + RNase T1
600
500
400
300
200
100
0
200
400
600
800

Figure 4

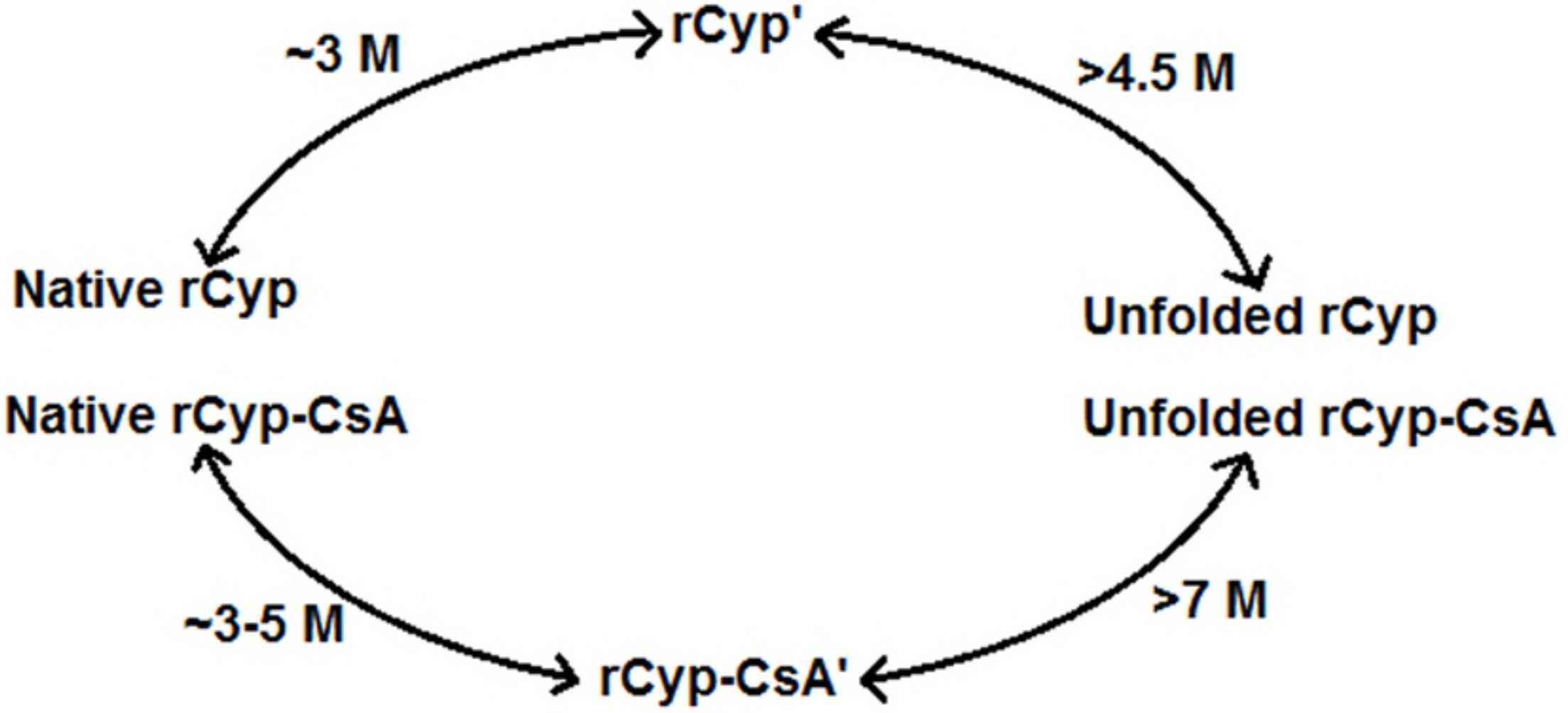
~3 M
rCyp'
>4.5 M
Native rCyp
Unfolded rCyp
Native rCyp-CsA
Unfolded rCyp-CsA
~3-5 M
rCyp-CsA'
>7 M

Figure 5

bioRxiv preprint doi: https://doi.org/10.1101/511048; this version posted January 3, 2019. The copyright holder for this preprint (which wa
certified by peer review) is the author/funder, who has granted bioRxiv a license to display the preprint in perpetuity. It is made available u
aCC-BY 4.0 International license.

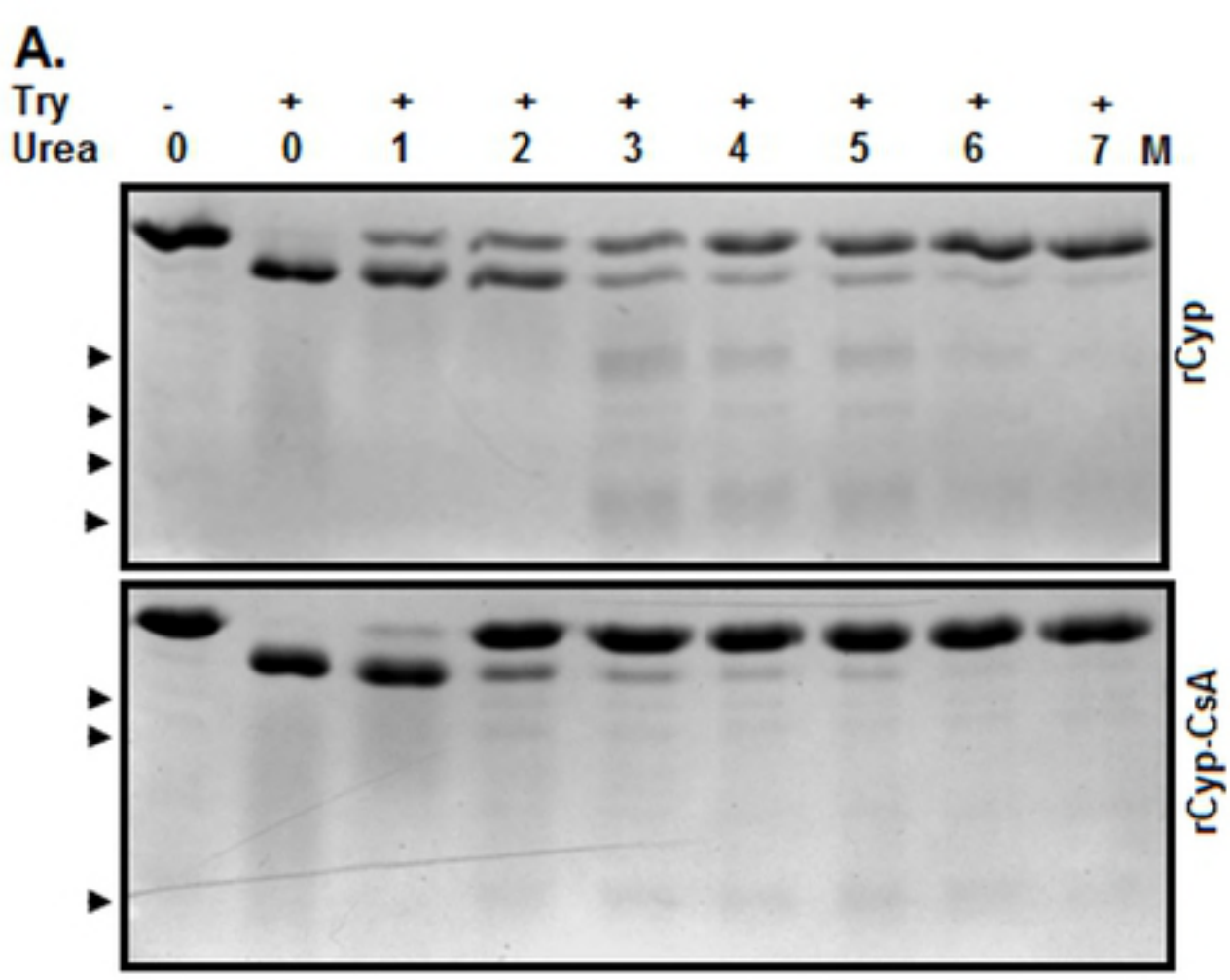

Figure 6